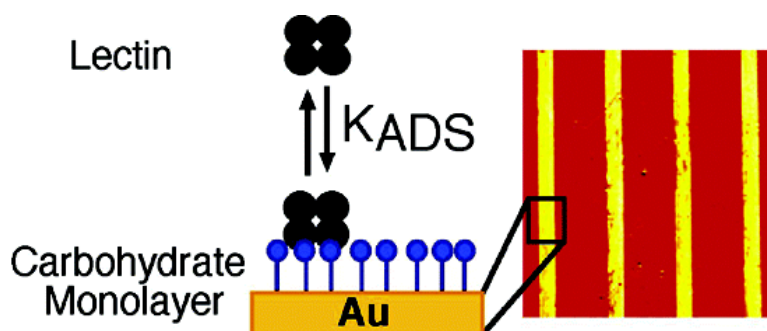


## Surface Plasmon Resonance Imaging Studies of Protein-Carbohydrate Interactions

Emily A. Smith, William D. Thomas, Laura L. Kiessling, and Robert M. Corn

*J. Am. Chem. Soc.*, **2003**, 125 (20), 6140-6148 • DOI: 10.1021/ja034165u • Publication Date (Web): 26 April 2003

Downloaded from <http://pubs.acs.org> on March 26, 2009



### More About This Article

Additional resources and features associated with this article are available within the HTML version:

- Supporting Information
- Links to the 48 articles that cite this article, as of the time of this article download
- Access to high resolution figures
- Links to articles and content related to this article
- Copyright permission to reproduce figures and/or text from this article

[View the Full Text HTML](#)



## Surface Plasmon Resonance Imaging Studies of Protein-Carbohydrate Interactions

Emily A. Smith, William D. Thomas, Laura L. Kiessling,\* and Robert M. Corn\*

Contribution from the Department of Chemistry, University of Wisconsin, 1101 University Ave., Madison, Wisconsin 53706, USA

Received January 14, 2003; E-mail: corn@chem.wisc.edu; kiessling@chem.wisc.edu

**Abstract:** Carbohydrate arrays fabricated on gold films were used to study carbohydrate-protein interactions with surface plasmon resonance (SPR) imaging. An immobilization scheme consisting of the formation of a surface disulfide bond was used to attach thiol-modified carbohydrates onto gold films and to fabricate carbohydrate arrays. The carbohydrate attachment steps were characterized using polarization modulation Fourier transform infrared reflection absorption spectroscopy; and poly(dimethylsiloxane) microchannels were used to immobilize probe compounds at discrete locations on a gold film. The binding of the carbohydrate-binding proteins concanavalin A (ConA) and jacalin to arrays composed of the monosaccharides mannose and galactose was monitored with SPR imaging. SPR imaging measurements were employed to accomplish the following: (i) construct adsorption isotherms for the interactions of ConA and jacalin to the carbohydrate surfaces, (ii) monitor protein binding to surfaces presenting different compositions of the immobilized carbohydrates, and (iii) measure the solution equilibrium dissociation constants for ConA and jacalin toward mannose and galactose, respectively. Adsorption coefficients ( $K_{\text{ADS}}$ ) of  $2.2 \pm 0.8 \times 10^7 \text{ M}^{-1}$  and  $5.6 \pm 1.7 \times 10^6 \text{ M}^{-1}$  were obtained for jacalin adsorbing to a galactose surface and ConA adsorbing to a mannose surface, respectively. The solution equilibrium dissociation ( $K_{\text{D}}$ ) constant for the interaction of jacalin and galactose was found to be  $16 \pm 5 \mu\text{M}$ , and for ConA and mannose was found to be  $200 \pm 50 \mu\text{M}$ .

### Introduction

Protein-carbohydrate interactions underlie many aspects of cellular recognition including cell adhesion, trafficking, apoptosis, and the immune response.<sup>1-3</sup> These specific interactions occur through glycoprotein, glycolipid, and polysaccharide displays found on cell surfaces and lectins, proteins with carbohydrate-binding domains.<sup>4</sup> Lectins typically possess shallow binding pockets that are solvent-exposed; therefore, the interaction between the carbohydrate and the protein is typically weak.<sup>5-7</sup> To provide interaction strength and specificity, many carbohydrate-binding proteins are oligomeric, consisting of several similar or identical monomers that each bind to a carbohydrate.<sup>1</sup> It is possible for the lectins to participate in multivalent binding, or the formation of several simultaneous binding events that provide an apparent binding affinity (functional affinity) that is greater than the sum of the individual interactions.

Tools for studying protein-carbohydrate interactions are necessary to gain an understanding of biological function and the roles these interactions play in disease states. Monovalent protein-carbohydrate interactions in solution are often of low affinity, which makes it difficult to analyze the binding

interactions using solution-based analysis methods such as those traditionally used to study protein or nucleic acid interactions.<sup>8</sup> Surface-based carbohydrate arrays can be used to facilitate the study of lectin recognition, and these will be valuable tools in the field of glycomics.<sup>9-13</sup> The presentation of carbohydrates in an array format provides a means to simultaneously monitor multiple binding events between immobilized carbohydrates and proteins binding from solution. In addition, carbohydrates immobilized on a surface are presented multivalently.<sup>14</sup> Lectin binding to a multivalent array is more avid and of higher specificity than the interactions of the monovalent counterparts.<sup>14-19</sup> Thus, immobilized arrays of ligands facilitate the analysis of lectin binding and can be relevant to cell surface presentations. To date, there are few reports<sup>9-13</sup> of the imple-

- (1) Lis, H.; Sharon, N. *Chem. Rev.* **1998**, *98*, 637-674.
- (2) Varki, A. *Glycobiology* **1993**, *3*, 97-130.
- (3) Bertozzi, C. R.; Kiessling, L. L. *Science* **2001**, *291*, 2357-2364.
- (4) Sharon, N.; Lis, H. *Science* **1989**, *246*, 227-246.
- (5) Kiessling, L. L.; Pohl, N. L. *Chem. Biol.* **1996**, *3*, 71-77.
- (6) Rini, J. M. *Curr. Opin. Struct. Biol.* **1995**, *5*, 617-621.
- (7) Weis, W. I.; Drickamer, K. *Annu. Rev. Biochem.* **1996**, *65*, 441-473.

- (8) Mann, D. A.; Kanai, M.; Maly, D. J.; Kiessling, L. L. *J. Am. Chem. Soc.* **1998**, *120*, 10 575-10 582.
- (9) Kiessling, L. L.; Cairo, C. W. *Nature Biotech.* **2002**, *20*, 234-235.
- (10) Wang, D.; Liu, S.; Trummer, B. J.; Deng, C.; Wang, A. *Nature Biotech.* **2002**, *20*, 275-281.
- (11) Fukui, S.; Feizi, T.; Galustian, C.; Lawson, A. M.; Chai, W. *Nature Biotech.* **2002**, *20*, 1011-1017.
- (12) Houseman, B. T.; Mrksich, M. *Chem. Biol.* **2002**, *9*, 443-454.
- (13) Fazio, F.; Bryan, M. C.; Blixt, O.; Paulson, J. C.; Wong, C.-H. *J. Am. Chem. Soc.* **2002**, *124*, 14 397-14 402.
- (14) Houseman, B. T.; Mrksich, M. *Top. Curr. Chem.* **2002**, *218*, 1-44.
- (15) Mortell, K. H.; Weatherman, R. V.; Kiessling, L. L. *J. Am. Chem. Soc.* **1996**, *118*, 2297-2298.
- (16) Lee, R. T.; Lee, Y. C. *Glycoconjugate J.* **1987**, *4*, 317.
- (17) Liang, R.; Yan, L.; Loebach, J.; Ge, M.; Uozumi, Y.; Sekanina, K.; Horan, N.; Gildersleeve, J.; Thompson, C.; Smith, A.; Biswas, K.; Still, W. C.; Kahne, D. *Science* **1996**, *274*, 1520-1522.
- (18) Liang, R.; Loebach, J.; Horan, N.; Ge, M.; Thompson, C.; Yan, L.; Kahne, D. *Proc. Natl. Acad. Sci. U.S.A.* **1997**, *94*, 10 554-10 559.
- (19) Lee, Y. C.; Lee, R. T. *Acc. Chem. Res.* **1995**, *28*, 321-327.

mentation of carbohydrate arrays due to the lack of robust, general, and controlled array fabrication strategies for carbohydrates.

In addition to the fabrication of carbohydrate arrays, a method to analyze protein binding to these arrays that does not require the use of fluorescent, radioactive, or enzymatic reporter groups is desirable. It is also desirable to circumvent the use of a secondary binding event for detection. We sought to employ surface plasmon resonance (SPR) imaging, an optical technique that is used to spatially monitor localized differences in the reflectivity of incident light from a prism-gold film interface that result from molecules adsorbing to or desorbing from the gold film. SPR imaging can be used to directly study the interactions of the carbohydrate arrays with proteins adsorbing from solution without the use of a reporter group.<sup>20–23</sup> In addition to the benefits afforded from the increased functional affinity and specificity of a surface-based assay format, the use of SPR to monitor protein–carbohydrate interactions with carbohydrate arrays has distinct advantages over fluorescence methods. Specifically, lower affinity interactions can be detected because SPR measurements can be made in the presence of a large excess of unbound protein, without the background problems that would complicate a similar measurement using fluorescence based techniques.

In this paper, we report the fabrication of mannose and galactose carbohydrate arrays on gold films using poly-(dimethylsiloxane) (PDMS) microchannels, and their subsequent use in SPR imaging experiments to monitor the binding of the lectins jacalin and concanavalin A (ConA). The attachment of the mannose and galactose ligands to the surface was characterized with polarization modulation Fourier transform infrared reflection absorption spectroscopy (PM-FTIRRAS). SPR imaging measurements were used to demonstrate that the immobilized carbohydrates are accessible to proteins in solution and that the lectin binding specificities could be detected. Adsorption isotherms for the binding of ConA and jacalin to carbohydrate surfaces were constructed to determine the adsorption coefficients ( $K_{\text{ADS}}$ ) for jacalin and ConA to the carbohydrate-substituted surfaces, and the binding of protein to surfaces presenting different carbohydrate compositions was studied. Finally, SPR imaging measurements were used to determine solution equilibrium dissociation constants ( $K_{\text{D}}$ ) using a model that was derived from the multivalent Scatchard analysis<sup>24</sup> and competition binding experiments, in which carbohydrate was present in solution with the protein.

## Experimental Methods

**Materials.** *N*-Succinimidyl *S*-acetylthiopropionate (SATP, Pierce), 2,2'-dipyridyl disulfide (DPDS, Aldrich), 11-mercaptoundecylamine (MUAM, Dojindo Laboratories), concanavalin A (ConA, Sigma), jacalin (Vector Laboratories), methyl  $\alpha$ -D-mannopyranoside (Sigma), methyl  $\alpha$ -D-galactopyranoside (Sigma), and *N*-hydroxysuccinimidyl ester of methoxypoly(ethylene glycol) propionic acid MW 2000 (Shearwater Polymers) were used as received. Experimental procedures

for the synthesis of compounds **1** and **2** are provided in the Supporting Information. Other standard chemicals were purchased from commercial suppliers, and used as received.

**Disulfide Attachment Chemistry.** The MUAM monolayer was prepared by soaking a gold-coated slide in a 1.0 mM MUAM in ethanol solution for at least 24 h. The reaction of the amine-substituted surface with the succinimide ester of SATP was carried out by treating the surface with 4.0 mM SATP in a mixture of dimethylformamide (DMF) and 0.1 M triethanolamine (10:90 DMF/triethanolamine) solution (pH 7.0) for 1–2 h. The thioester was cleaved by soaking the slide for 20 min in a solution of 0.5 M hydroxylamine, 0.05 M dithiothreitol (DTT), 0.05 M phosphate buffer and 0.025 M EDTA at pH 7.5 to generate the free thiol. To generate the intermediate mixed disulfide, the thiol-substituted surface was treated with 2,2'-dipyridyl disulfide (1 mg/mL) in a 1:1 mixture of 0.1 M triethanolamine (pH 8.0) and DMF for 2 h. Immobilization of the carbohydrate derivatives, compounds **1** and **2**, was carried out in 20 mM phosphate buffer (pH 7.5, 100 mM NaCl, 5 mM  $\text{MgCl}_2$ ) for 12 h. Between each reaction step the slides were thoroughly rinsed with water and dried under a nitrogen stream.

**PM-FTIRRAS Surface Characterization.** Commercial gold slides (5 nm Cr and 100 nm Au) were purchased from Evaporated Metal Films (New York) and were used for all PM-FTIRRAS measurements. Mid-IR spectra were collected using a Mattson RS-1 spectrometer with real-time interferogram sampling electronics and optical layout, as previously described.<sup>25,26</sup> Spectra were collected from 1000 scans with a resolution of 4  $\text{cm}^{-1}$  using a narrow-band HgCdTe detector. Spectra from the CH stretching region were collected using a Bruker Vector-22 spectrometer with the same sampling electronics and optical layout as described above. Spectra were collected from 1000 scans with a resolution of 2  $\text{cm}^{-1}$  using an InSb detector.

**Surface Plasmon Resonance Imaging.** Gold films (45 nm) with a thin chromium underlayer (1 nm) used to construct the arrays were vapor-deposited on SF10 glass slides (Schott Glass Technologies) in a Denton Vacuum DV-502A evaporator. The in situ SPR imaging apparatus has been described elsewhere.<sup>22,27,28</sup> Briefly, p-polarized collimated white light was directed toward a prism/Au thin film/buffer assembly at a fixed angle. Light reflected from this assembly was passed through a narrow band-pass filter ( $\lambda = 800$  nm) and collected by a CCD camera. The carbohydrate arrays were imaged in 25 mM tris-(hydroxymethyl) aminomethane hydrochloride buffer (pH 7.6, 124 mM NaCl, 25 mM  $\text{CaCl}_2$ , 5 mM MnCl).

**Data Analysis.** All SPR Images were collected using the software program XCAP v1.0 (EPIX Inc.). Further image analysis was performed using the NIH Image v.1.61 software package. The line profile option from this software was used to measure the signal (in pixel values) from an SPR image, and this was subsequently converted to percent reflectivity values. The error bars indicated in the figures show the average percent error for all data points reported in the figure.

In section (F) of the Results and Discussion section, competitive binding experiments are used to determine the  $K_{\text{D}}$  values for lectin-carbohydrate binding interactions. A multivalent Scatchard analysis is used to characterize the interactions of multivalent acceptors with multivalent ligands.<sup>24</sup> This analysis can be used to construct an expression for the equilibrium dissociation constant for the interaction of a multivalent acceptor with a monovalent ligand under the experimental conditions used in this study. In the following analysis, the assumption is made that each acceptor site acts independently of the other sites.

(20) Brockman, J. M.; Nelson, B. P.; Corn, R. M. *Annu. Rev. Phys. Chem.* **2000**, *51*, 41–63.

(21) Frutos, A. G.; Corn, R. M. *Anal. Chem.* **1998**, *70*, 449A–455A.

(22) Brockman, J. M.; Frutos, A. G.; Corn, R. M. *J. Am. Chem. Soc.* **1999**, *121*, 8044–8051.

(23) Nelson, B. P.; Grimsrud, T. E.; Liles, M. R.; Goodman, R. M.; Corn, R. M. *Anal. Chem.* **2001**, *73*, 1–7.

(24) Harris, S. J.; Jackson, C. M.; Winzor, D. J. *Arch. Biochem. Biophys.* **1995**, *316*, 20–23.

(25) Green, M. J.; Barner, B. J.; Corn, R. M. *Rev. Sci. Instrum.* **1991**, *62*, 1426–1430.

(26) Barner, B. J.; Green, M. J.; Saez, E. I.; Corn, R. M. *Anal. Chem.* **1991**, *63*, 55–60.

(27) Jordan, C. E.; Frutos, A. G.; Thiel, A. J.; Corn, R. M. *Anal. Chem.* **1997**, *69*, 4939–4947.

(28) Nelson, B. P.; Frutos, A. G.; Brockman, J. M.; Corn, R. M. *Anal. Chem.* **1999**, *71*, 3928–3934.

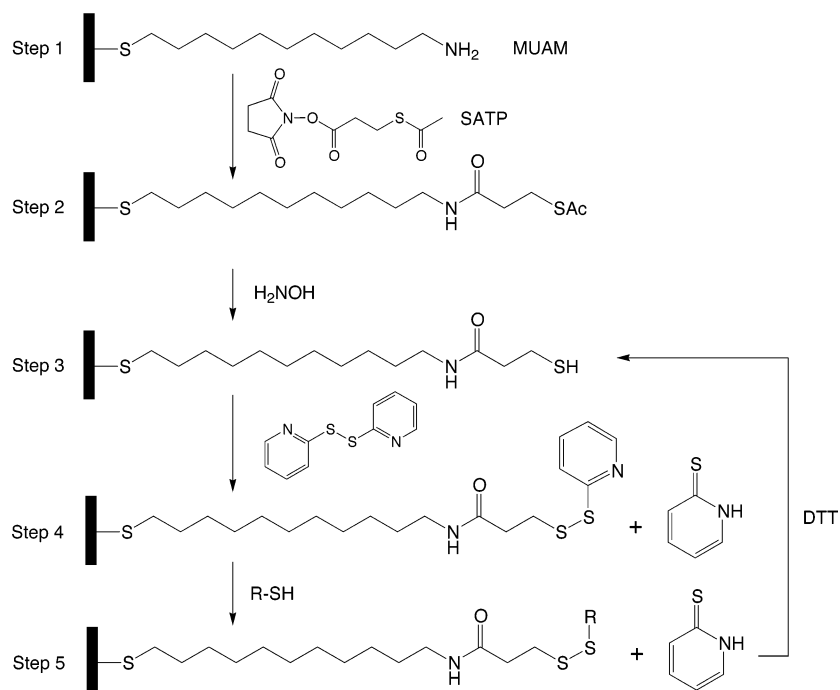


**Figure 1.** Schematic presentation of the surface modification process with SATP: (Step 1) MUAM surface; (Step 2) thiolation with SATP; (Step 3) sulfhydryl deprotection; (Step 4) activated sulfhydryl surface with pyridyl groups; (Step 5) exchange reactions between the pyridyl disulfide surface and sulfhydryl-containing carbohydrate derivative (R-SH) in solution, which produces the leaving group pyridine-2-thione. When the surface (Step 5) is exposed to DTT, the disulfide linkage is cleaved. The immobilized molecule is released and the free sulfhydryl surface (Step 3) is regenerated.

The interaction between a monovalent ligand (L), and one acceptor binding site (A) on a multivalent protein (P) can be represented as



The expression for the equilibrium dissociation constant for this interaction is

$$K_D = \frac{[\text{L}][\text{A}]}{[\text{LA}]} \quad (1)$$

where [LA] is the concentration of acceptor/ligand complexes, [A] is the concentration of free acceptor sites, and [L] is the concentration of free ligand. The concentration of total acceptor sites,  $[\text{A}_0]$ , is equal to the concentration of free acceptor sites plus the concentration of acceptor/ligand complexes

$$[\text{A}_0] = [\text{A}] + [\text{LA}] \quad (2)$$

substituting this into eq 1

$$K_D = \frac{[\text{A}][\text{L}]}{[\text{A}_0] - [\text{A}]} \quad (3)$$

In surface competition experiments the total protein concentration  $[\text{P}_0]$  is constant, and the SPR response and adsorption isotherm are used to determine the equivalent free protein concentration [P] as the amount of ligand is increased. The concentration of the free acceptor sites in solution, [A], is equal to  $q[\text{P}]$ , where  $q$  is the number of binding sites on a protein. Likewise, the total concentration of acceptor sites  $[\text{A}_0]$  is equal to  $q[\text{P}_0]$ . Substituting these values into eq 3 yields

$$K_D = \frac{q[\text{P}][\text{L}]}{q[\text{P}_0] - q[\text{P}]} = \frac{[\text{P}][\text{L}]}{[\text{P}_0] - [\text{P}]} \quad (4)$$

If the initial concentration of ligand is much greater than the initial concentration of protein ( $[\text{L}_0] \gg [\text{P}_0]$ ), then the concentration of free ligand is approximately the concentration of initial ligand ( $[\text{L}] \approx [\text{L}_0]$ ),

and the resulting expression for the equilibrium dissociation constant is

$$K_D = \frac{[\text{P}][\text{L}_0]}{[\text{P}_0] - [\text{P}]} \quad (5)$$

To determine  $K_D$ , the SPR imaging data is used to measure [P] for known values of  $[\text{P}_0]$  and  $[\text{L}_0]$ .

## Results and Discussion

**A. Carbohydrate Surface Attachment Chemistry and Surface Monolayer Characterization.** To attach carbohydrate derivatives to the surface, we chose to use a disulfide linkage which has been previously shown to be effective for immobilizing thiol-modified oligonucleotides<sup>29</sup> and peptides<sup>30</sup> onto gold surfaces. The reaction scheme that was used is depicted in Figure 1. A densely packed self-assembled monolayer of an amine-terminated alkanethiol is first generated (MUAM, step 1), and a series of successive reactions is used to modify this monolayer via covalent bond formation. The MUAM surface is treated with the heterobifunctional cross-linker *S*-acetylthiopropionate, which contains an amine-reactive succinimide ester and a protected thiol moiety. Reaction of the succinimide ester group with the primary amine on MUAM results in the formation of an amide bond to yield a monolayer with masked thiol groups (Step 2). The thioester can be transformed to yield a free sulfhydryl surface with an effective nucleophile, such as hydroxylamine (Step 3). These reaction steps have been characterized with PM-FITRRAS.<sup>29</sup>

To implement the disulfide attachment strategy for carbohydrates, derivatives containing thiol groups needed to be gener-

(29) Smith, E. A.; Wanat, M. J.; Cheng, Y.; Barreira, S. V. P.; Frutos, A. G.; Corn, R. M. *Langmuir* **2001**, *17*, 2502–2507.

(30) Wegner, G. J.; Lee, H. J.; Corn, R. M. *Anal. Chem.* **2002**, *74*, 5161–5168.

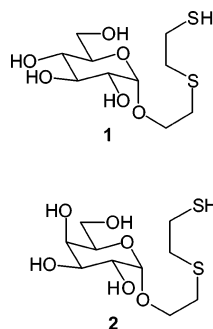


**Figure 2.** Structure of the  $\alpha$ -mannose (**1**) and  $\alpha$ -galactose (**2**) derivatives used in this study. Both were synthesized to contain an anomeric linker with a free sulfhydryl group. The complete synthesis and characterization details are provided in the Supporting Information.

**Table 1.** PM-FTIRRAS Band Assignment of Surface Modification with Carbohydrate Probes

surface	wavenumber ( $\text{cm}^{-1}$ )	assignment
mannose or galactose derivative	3334 (broad)	OH stretching vibrations
	2928	$\text{CH}_2$ asymmetrical stretch
	2855	$\text{CH}_2$ symmetrical stretch
	1261	$\text{CH}_2$ twisting mode
	1191	CO stretch of cyclic ether
	1107	CO stretch of dialkyl ether

ated. We chose to append a thiol-containing linker at the anomeric position. This site is a logical position for attachment as it is used for naturally occurring glycoconjugates. The mannose (**1**) and galactose (**2**) derivatives used in this study were selected because they interact with different well-characterized lectins (Figure 2). Specifically,  $\alpha$ -linked mannose derivatives bind to ConA, but galactose ligands do not.<sup>8</sup> In contrast, the lectin jacalin interacts preferentially with  $\alpha$ -linked galactose over mannose derivatives.<sup>31</sup> By using derivatives **1** and **2**, the ability of SPR imaging to distinguish specific carbohydrate-protein interactions can be determined.

With the carbohydrate derivatives in hand, a two-step reaction is used to attach thiol-containing carbohydrates onto the sulfhydryl-terminated surface. The first step involves the formation of an immobilized mixed disulfide via reaction of the surface sulfhydryl groups and 2,2'-dipyridyl disulfide in solution (Step 4). The target compounds could then be appended through a thiol-disulfide exchange reaction between the thiol-containing carbohydrate and the surface disulfide (Step 5). The pyridine-2-thione released in this process is a better leaving group than the surface or the carbohydrate-containing thiolate; thus, the desired disulfide is formed preferentially.<sup>32</sup> The surface density of immobilized ligands obtained with this attachment chemistry is approximately  $10^{13}$  molecules/ $\text{cm}^2$ . This surface density is similar to that obtained in the attachment of peptides to gold surfaces using the disulfide attachment chemistry.<sup>30</sup>

PM-FTIRRAS spectra from the Mid-IR and CH stretching regions ( $2500\text{--}3500\text{ cm}^{-1}$ ) were acquired to verify the attachment of these carbohydrate derivatives to the surface. Table 1 lists the FTIR peak assignments in the Mid-IR and CH stretching regions for the spectra obtained upon attaching compounds **1** and **2** to the surface using the disulfide linkage. The broad peak at  $3334\text{ cm}^{-1}$  has been assigned to the OH stretching vibrations

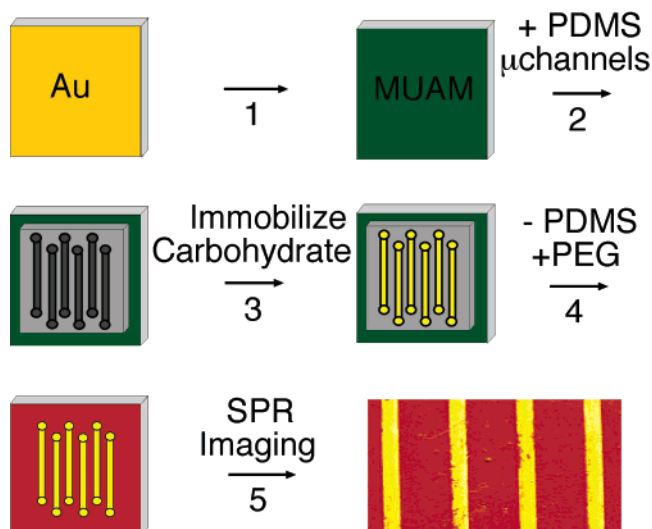


**Figure 3.** Schematic presentation of the five-step process used to fabricate carbohydrate arrays using PDMS microchannels to pattern the gold surface. (Step 1) A thin gold film is immersed in an ethanolic solution of amine-terminated alkanethiol to form a packed monolayer. (Step 2) PDMS microchannels are placed on the gold surface. (Step 3) The carbohydrate ligands are immobilized on the surface of the gold film using the attachment chemistry presented in Figure 1. (Step 4) After immobilizing the carbohydrate, the PDMS is removed from the surface. The entire surface is then reacted with a succinimide ester derivative of PEG to form a background monolayer that resists the nonspecific adsorption of proteins from solution. (Step 5) The interaction of the array with proteins in solution is monitored with SPR imaging. Shown in the lower right corner is a typical SPR image of an array fabricated using PDMS microchannels. Each yellow line corresponds to one array element consisting of a unique carbohydrate or mixture of carbohydrates.

from the sugar hydroxyl groups. Bands at  $2928$  and  $2855\text{ cm}^{-1}$  were assigned to the  $\text{CH}_2$  asymmetric and symmetric stretching modes of the linker, respectively. In the Mid-IR region, peaks centered at  $1261\text{ cm}^{-1}$  were assigned to the  $\text{CH}_2$  twisting modes. The bands at  $1191$  and  $1107\text{ cm}^{-1}$  have been assigned to the CO stretch of the cyclic ether in the sugar ring and the CO stretch of the dialkyl ether in the linker attachment, respectively.

**B. Fabrication of Mannose and Galactose Arrays.** Mannose and galactose arrays were fabricated using a combination of the disulfide surface attachment chemistry and PDMS microchannels to pattern the surface (Figure 3). To generate the array, a MUAM monolayer was formed on the gold film (Figure 3, Step 1). PDMS microchannels that had been fabricated using a 3-D silicon mask were placed on the surface (Figure 3, Step 2).<sup>33</sup> These microchannels were composed of a series of parallel channels, each with a width of  $300\text{ }\mu\text{m}$ , that had entrance and exit reservoirs at their ends for sample introduction. Immobilization of the carbohydrates was carried out in the channels by flowing  $1\text{ }\mu\text{L}$  of solution through the channels. Because each channel was independent, a different carbohydrate or mixture of carbohydrates could be introduced and immobilized within each channel (Figure 3, step 3). After carbohydrate attachment, the PDMS microchannels were removed from the modified surface. The number of species that can be immobilized in this manner depends on the number of channels fabricated. To date, up to 10 species have been immobilized on a gold surface using this technique; however, as many as 150 species can be immobilized on the same gold

(31) Bourne, Y.; Astoul, C. H.; Zamboni, V.; Peumans, W. J.; Menu-Bouaouiche, L.; Van Damme, E. J. M.; Barre, A.; Rouge, P. *Biochem. J.* **2002**, *364*, 173–180.

(32) Grasetti, D. R.; Murray, J. F. *J. Anal. Biochem.* **1967**, *21*, 427.

(33) Lee, H. J.; Goodrich, T. T.; Corn, R. M. *Anal. Chem.* **2001**, *73*, 5525–5531.

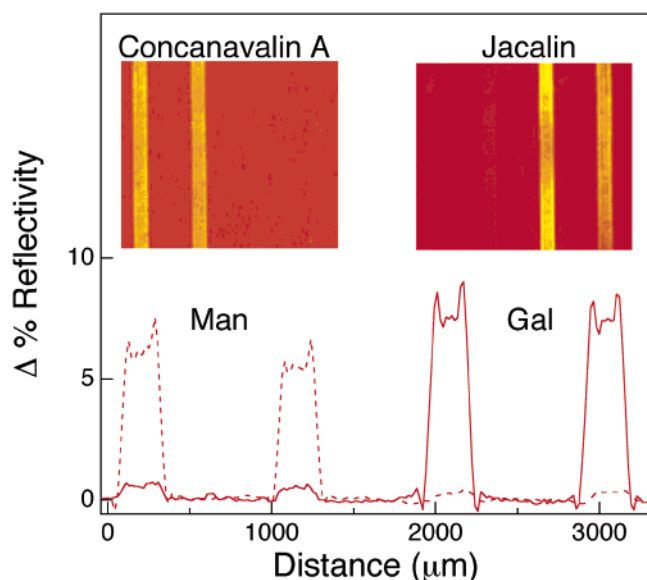


**Figure 4.** Line profiles taken from SPR difference images of a two-component carbohydrate array with two (left) channels containing compound 1 and two (right) channels containing compound 2. The SPR image on the left and dotted line profile below correspond to the introduction of the lectin ConA to the surface and show the binding of ConA to the mannose array elements. The SPR image on the right and solid line profile correspond to the introduction of the lectin jacalin to the surface and show the binding of jacalin to the galactose array elements.

film (1.8 × 1.8 cm) by reducing the channel width and the space between the channels.<sup>33</sup>

To form an array background that is resistant to protein adsorption, the entire surface was exposed to a solution of the succinimide ester of poly(ethylene glycol) in phosphate buffer (pH 8.0). The succinimide ester reacts with unmodified amine groups to generate a surface covered in poly(ethylene glycol) groups (Figure 3, step 4). Such surfaces have been shown to resist nonspecific protein adsorption.<sup>34–36</sup> The resulting array was then placed into a flow cell for SPR imaging experiments. A typical SPR image of a four-component carbohydrate array is shown in Figure 3 (Figure 3, step 5).

To determine whether the carbohydrates immobilized using the disulfide attachment chemistry are accessible to proteins in solution, a two-component carbohydrate array was fabricated. The resulting array, which contains two channels of the mannose derivative (1), and two channels of the galactose derivative (2) was exposed to the lectins ConA and jacalin. As mentioned previously, the lectin ConA exhibits selectivity for mannose over galactose residues;<sup>8</sup> jacalin binds to both galactose and mannose, but it binds to mannose residues with several orders of magnitude lower affinity than to galactose residues.<sup>31</sup> Shown in Figure 4 are two SPR difference images, obtained by subtracting the images taken before and after the protein adsorption events, and the corresponding line profiles taken from these SPR images. The image on the left and corresponding line profile (dotted line) were obtained upon exposing the array to a 200 nM solution of ConA. The data indicate that the protein binds selectively to the mannose array elements.

The carbohydrate arrays fabricated with this attachment chemistry were robust, and could be used in approximately 20 binding cycles before degradation of the surface was observed. The arrays were regenerated by treatment with a high pH buffer solution (pH 11.5) and/or high concentration salt solutions to remove the bound lectin. The major factor limiting the use of these arrays in additional binding experiments is the slow accumulation of nonspecifically adsorbed protein onto the surface. The image shown on the right in Figure 4 and corresponding line profile (solid line) were obtained after removing the ConA from the surface and exposing the array to a 100 nM solution of the lectin jacalin. In contrast to ConA, jacalin was found to bind selectively to the galactose derivative. The selectivity of ConA and jacalin toward the immobilized carbohydrates demonstrates that this immobilization method affords surfaces suitable for assessing the protein binding specificity for carbohydrates.

There are three factors that can influence the interaction between the adsorbing protein and the carbohydrate surface: protein–protein interactions between adsorbing protein molecules, the carbohydrate surface site density, and the number of interactions occurring between the adsorbing protein and the carbohydrate surface. The protein–protein interactions were studied using adsorption isotherms (section C). To study the effect of the surface site density on protein adsorption, the composition of the active carbohydrate immobilized on the surface was varied (section D). Finally, the effect of multivalent protein binding to the surface was studied by constructing adsorption isotherms for surfaces with varying carbohydrate compositions (section E).

**C. Adsorption Coefficients for the Binding of Jacalin to Galactose Surfaces and ConA to Mannose Surfaces.** To study the interaction strength between the immobilized carbohydrates and ConA or jacalin, adsorption isotherms for these lectins interacting with carbohydrate arrays were constructed by monitoring the protein surface coverage as a function of protein concentration. Thermodynamic data suggest that the binding affinity of jacalin to methyl- $\alpha$ -D-galactopyranoside ( $\alpha$ -MeGal,  $K_D = 25 \mu\text{M}$ )<sup>37</sup> is higher than that for ConA binding to methyl- $\alpha$ -D-mannopyranoside ( $\alpha$ -MeMan,  $K_D = 130 \mu\text{M}$ ).<sup>38</sup> Consequently, we sought to determine if differences in protein adsorption could be detected.

It has been previously shown that SPR imaging can be used to quantitate the amount of material adsorbing to a gold surface; thereby providing a measure of protein surface coverage.<sup>23</sup> The adsorption isotherms for the binding of (Figure 5, circles) ConA to a mannose surface, and (Figure 5, squares) the binding of jacalin to a galactose surface were obtained by plotting the relative protein surface coverage at equilibrium as a function of the protein concentration. The solid lines in Figure 5 were obtained by fitting the data to a Frumkin isotherm, which has the form

$$[P] = K_{\text{ADS}}^{-1} \frac{\theta}{1 - \theta} e^{-2a\theta} \quad (6)$$

where [P] is the concentration of protein in solution,  $K_{\text{ADS}}$  is

(34) Silin, V.; Weetall, H.; Vanderah, D. J. *J. Coll. Inter. Sci.* **1997**, *185*, 94–103.

(35) Ostuni, E.; Chapman, R. G.; Holmlin, R. E.; Takayama, S.; Whitesides, G. M. *Langmuir* **2001**, *17*, 5605–5620.

(36) Harder, P.; Grunze, M.; Dahint, R.; Whiteside, G. M.; Laibinis, P. E. *J. Phys. Chem. B* **1998**, *102*, 426–436.

(37) Mahanta, S. K.; Sastry, M. V.; Surolia, A. *Biochem. J.* **1990**, *265*, 831–840.

(38) Weatherman, R. V.; Mortell, K. H.; Chervenak, M.; Kiessling, L. L.; Toone, E. J. *Biochem.* **1996**, *35*, 3619–3624.

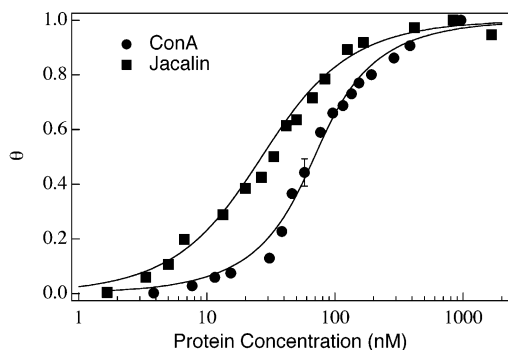


**Figure 5.** Plots of the relative protein surface coverage (fraction of occupied surface sites,  $\theta$ ) as determined by SPR imaging as a function of the protein concentration in the solution. The data shown correspond to (squares) the binding of jacalin to a galactose surface and (circles) the binding of ConA to a mannose surface. The data have been fit to Frumkin isotherms (solid lines).

the adsorption coefficient,  $\theta$  is the protein surface coverage (given by  $\Gamma/\Gamma_{\text{MAX}}$ ), and  $a$  is the Frumkin interaction parameter.<sup>39</sup> The Frumkin interaction parameter in eq 6 indicates whether the adsorbing molecules exhibit attractive or repulsive (lateral) interactions. When  $a$  is equal to zero in eq 6, the Langmuir adsorption isotherm is obtained. Positive Frumkin interaction parameters were obtained from the fits of the lectin isotherms shown in Figure 5, and this indicates attractive forces are present between the adsorbing protein molecules. The adsorption coefficient provides information about the strength of the interaction between the adsorbing species and the species on the surface. The adsorption coefficient for jacalin binding to the galactose-substituted surface was found to be  $2.2 \pm 0.8 \times 10^7 \text{ M}^{-1}$ , whereas that for the interaction of ConA and the mannose-derivatized surface was found to be  $5.6 \pm 1.7 \times 10^6 \text{ M}^{-1}$ . The adsorption coefficients indicate that the interaction between jacalin and the surface immobilized galactose is stronger than the interaction between ConA and the surface immobilized mannose, which is consistent with the aforementioned thermodynamic data.

**D. Mixed Galactose and Mannose Monolayers.** Both ConA and jacalin are tetrameric proteins, with 4 carbohydrate-binding sites. Thus, we envisioned that these proteins might engage in multivalent interactions with the appropriate surfaces. To study multivalent binding between the lectin and the surface, SPR imaging was used to monitor the binding of ConA and jacalin to surfaces that presented varying compositions of immobilized carbohydrates. The composition of the immobilized carbohydrate surfaces can be controlled using the disulfide attachment scheme by varying the concentration of the carbohydrate derivatives that are conjugated to the surface (Figure 3, step 3). The active carbohydrate derivative (e.g., compound **1** for ConA) can be diluted with a nonactive species (e.g., compound **2** for ConA). We choose to use carbohydrates for both the “active” and “inactive” epitopes as the sterics of the surface should not be altered. Thus, adsorption data can be more readily compared.<sup>40</sup> Shown in Figure 6 are the normalized SPR signals obtained for the binding of (squares) ConA and (triangles) jacalin to mixed carbohydrate monolayers, composed of mixtures of mannose and galactose ligands. The amount of mannose or

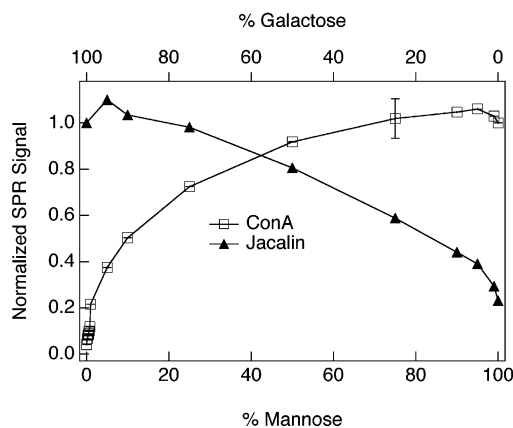


**Figure 6.** Plots showing the normalized SPR signal obtained for (square) ConA and (triangle) jacalin binding to surfaces with the indicated compositions of mannose and galactose derivatives. See text for further discussion.

galactose immobilized on the surface varied in these studies, however the total amount of carbohydrate remained constant. For example, the 0% mannose surface contained 100% galactose, and the 50% mannose surface contained 50% galactose. The data provide insight into the interactions of the lectins with the carbohydrate-modified surfaces.

The binding of either ConA or jacalin to the surface could be detected by SPR imaging, even for very low surface compositions of active carbohydrate. For ConA, protein binding to surfaces composed of 0.2% mannose was detected. In addition, there is a linear relationship between the amount of protein adsorbed to the surface and the mannose composition for the binding of ConA to surfaces presenting low mannose compositions (0 to 1% mannose). For surfaces with compositions of mannose greater than 1%, the relationship is no longer linear. The binding of a 150 nM solution of jacalin to 0% galactose surfaces showed that a small but significant amount of protein adsorbed to the surface; this binding was not observed at low (below 100 nM) jacalin concentrations. This result is consistent with reports that jacalin has a low affinity for mannose, albeit an affinity that is several orders of magnitude lower than its affinity for galactose. In contrast, no significant ConA binding to the 0% mannose surface occurs even at a ConA concentration of 300 nM.

The data also indicate that there is a plateau in the amount of ConA or jacalin adsorbing to the surface as the amount of active carbohydrate on the surface increases (Figure 6). These experiments were performed at protein concentrations corresponding to less than a full monolayer of protein (300 nM ConA and 150 nM jacalin) for the 100% mannose and galactose surfaces. Therefore, the plateau in protein adsorption cannot be explained by steric constraints between adsorbed protein molecules that would limit the amount of protein that adsorbs to the surface. In addition, it has been previously shown by SPR imaging that the binding of antibody from solution onto mixed peptide monolayers containing a peptide sequence recognized by the antibody results in a linear relationship between the amount of antibody binding to the surface and the amount of active peptide immobilized on the surface.<sup>30</sup>

The plateau in protein binding seen in Figure 6 indicates that there is a density of immobilized carbohydrate ligands beyond which the addition of more binding epitopes does not increase the adsorption of protein to the surface. This result suggests

(39) Adamson, A. W.; Gast, A. P. *Physical Chemistry of Surfaces*; John Wiley & Sons Inc.: New York, 1997.

(40) Cairo, C. W.; Gestwicki, J. E.; Kanai, M.; Kiessling, L. L. *J. Am. Chem. Soc.* **2002**, *124*, 1615–1619.

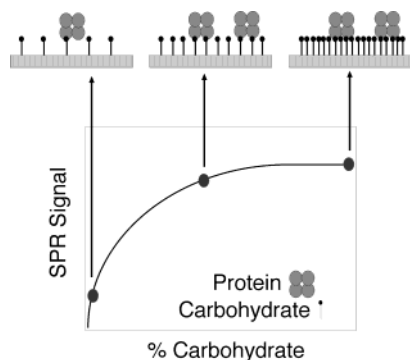


**Figure 7.** Schematic model of the data shown in Figure 6. For a low level of ligand substitution on the surface, the spacing between the carbohydrate binding sites on the protein prohibits the protein from binding to more than one immobilized carbohydrate epitope. At an intermediate ligand density, the spacing of the carbohydrates on the surface allows the protein to interact with multiple carbohydrates on the surface. At a high carbohydrate coverage, immobilization additional carbohydrates does not increase the amount of protein bound to the surface.

that at high ligand densities not all of the carbohydrate residues at high mannose- (ConA) or galactose-derivatized (jacalin) surfaces are active. This observation can be explained by the distance between the carbohydrate binding domains on the lectins and the density of the immobilized carbohydrates on the surface. For example, ConA is capable of forming two attachment points to the surface, and the distance between these points on the protein is approximately 6.5 nm.<sup>41</sup> On the basis of the surface density of ligands immobilized using the disulfide attachment chemistry for 10%, 50%, and 100% mannose surfaces, for example, the approximate distance between mannose residues is 11, 5, and 4 nm, respectively. For a 10% mannose-substituted surface, the average distance between immobilized mannose residues is too great for adsorbed ConA to be interacting with more than one mannose residue (Figure 7, left). Near 50% mannose substitution, the mannose residues are close enough on the surface such that on average an adsorbed ConA can bind to two mannose residues (Figure 7, center). When the level of mannose-substitution is 100%, there are more than 2 carbohydrate derivatives available on the surface within the carbohydrate binding region of each protein; however, each protein can only interact with 2 mannose residues at one time (Figure 7, right). No further protein can adsorb to the surface even though some mannose residues remain unoccupied due to the limitations on the carbohydrate binding site density.

**E. Adsorption Isotherms for Lectin binding to 10%, 50%, and 100% Carbohydrate Surfaces.** To determine if the interaction strength between the adsorbed protein and the surface changes as the amount of carbohydrate ligand on the surface increases, the adsorption isotherms for jacalin and ConA were constructed for surfaces composed of 10%, 50%, and 100% carbohydrate ligand. If the lectins engage in multivalent binding with the surface at high levels of ligand substitution, then the interaction strength between the lectin and the surface should increase as the percentage of ligand increases. The adsorption isotherms for jacalin binding to (triangles) 10%, (squares) 50%, and (circles) 100% galactose surfaces (Figure 8) were fit to Frumkin isotherms (eq 6), and the Frumkin interaction parameters and adsorption coefficients obtained from these data are

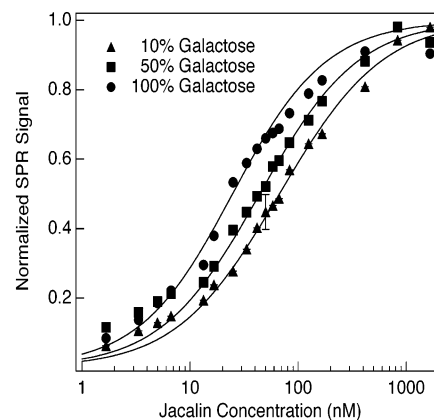


**Figure 8.** Isotherms for jacalin binding to (triangle) 10%; (square) 50%; and (circle) 100% galactose-modified surfaces. Each set of data has been normalized to the maximum signal obtained for that surface, and was fit using the Frumkin isotherm equation. Shown in Table 2 are the Frumkin interaction parameters and adsorption coefficients for jacalin interacting with these surfaces.

**Table 2.** Langmuir Adsorption Coefficients ( $K_{\text{ADS}}$ ), and Frumkin Interaction Parameters

protein	surface composition	$K_{\text{ADS}}$	$a$
jacalin	100% galactose	$2.2 \pm 0.8 \times 10^7 \text{ M}^{-1}$	$0.5 \pm 0.3$
	50% galactose	$1.6 \times 10^7 \text{ M}^{-1}$	0.4
	10% galactose	$1.2 \times 10^7 \text{ M}^{-1}$	0.4
ConA	100% mannose	$5.6 \pm 1.7 \times 10^6 \text{ M}^{-1}$	0.55
	50% mannose	$5.6 \times 10^6 \text{ M}^{-1}$	0.55
	10% mannose	$5.0 \times 10^6 \text{ M}^{-1}$	0

listed in Table 2. The adsorption coefficients indicate that the interaction between jacalin and the surface becomes stronger as the amount of immobilized galactose increases on the surface.

The adsorption isotherms for ConA binding to 10%, 50%, and 100% mannose surfaces show similar trends to the jacalin adsorption isotherms (Table 2). The interaction strength increases between ConA and the mannose-substituted surface upon increasing the composition of mannose from 10% to 50%. The adsorption coefficient remains constant, within experimental error, as the mannose composition is further increased to 100%. The increase in  $K_{\text{ADS}}$  for surfaces presenting high densities of active carbohydrate imply that at high active carbohydrate densities, the lectins are interacting with the surface through multivalent interactions, and that the extent of multivalent binding increases as the surface density of active carbohydrate increases.

**F. Solution Equilibrium Dissociation Constants of Carbohydrate-Lectin Interactions Measured with SPR Imaging.** It is possible to determine the solution equilibrium dissociation constants ( $K_{\text{D}}$ ) for carbohydrate lectin interactions using the SPR imaging technique to probe the concentration of unbound protein in the presence of carbohydrate in solution. This analysis allows for the direct comparison of affinity measurements obtained with SPR imaging and solution based affinity measurements.

In a competitive binding experiment, carbohydrates in solution compete with the immobilized carbohydrate ligands for binding sites on the lectin, establishing a coupled equilibrium between the binding of the protein to the surface immobilized species and to the species present in solution. This is schematically represented in the inset to Figure 9. The total concentration of

(41) Bittiger, H.; Schnebli, H. P. *Concanavalin A as a Tool*; John Wiley and Sons: London, New York, 1976.



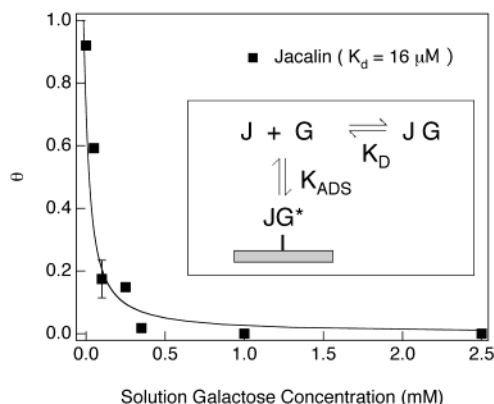


**Figure 9.** Plot of the relative surface coverage of jacalin, measured with SPR imaging, as a function of the concentration of  $\alpha$ -MeGal in solution. The  $\alpha$ -MeGal in solution competes with the surface immobilized galactose for the jacalin binding sites through a coupled equilibrium shown in the figure inset. The figure inset has been simplified to show jacalin binding to one galactose molecule from solution; however, jacalin has four galactose binding sites. The data are fit as discussed in the text, using eqs 5 and 6, to determine the solution dissociation constant  $K_D$ .

protein ( $[P_o]$ ) is held constant, while the concentration of carbohydrate in solution ( $[L_o]$ ) is increased. An associated decrease in the amount of protein binding to the surface is observed, which is monitored by SPR imaging (Figure 9). Using the SPR imaging signal, the unbound protein concentration ( $[P]$ ) can be obtained via the adsorption isotherm (eq 6). Once the concentration of  $P$  has been measured, it is possible to determine  $K_D$  using eq 5, which is derived from the multivalent Scatchard formula.<sup>24</sup> This analysis makes three assumptions: (i) the amount of protein binding to the sensor surface is negligible compared to the total amount of protein in the system, (ii) the initial concentration of ligand is much greater than the initial concentration of protein so that the concentration of unbound ligand is approximately equal to the total concentration of ligand ( $[L_o] \approx [L]$ ), and (iii) each monomer in the protein binds to the ligand independently of the other monomers. A competition binding experiment was performed with jacalin binding to a 1% galactose surface using  $\alpha$ -MeGal in solution as the competitor ligand (Figure 9). When the data is analyzed according to eqs 5 and 6, a  $K_D$  value of  $16 \pm 5 \mu\text{M}$  for jacalin and  $\alpha$ -MeGal was obtained. This value agrees well with the solution dissociation constant for jacalin binding to  $\alpha$ -MeGal, which is  $25 \mu\text{M}$ .<sup>37</sup> The results for an inhibition binding experiment performed for the binding of ConA to a 10% mannose surface with increasing concentration of  $\alpha$ -MeMan in solution are shown in Figure 10. An equilibrium dissociation constant of  $200 \pm 50 \mu\text{M}$  was obtained from this experiment. This value correlates well with the dissociation constant of  $130 \mu\text{M}$  for  $\alpha$ -MeMan obtained by microcalorimetry for the interaction of ConA with mannose.<sup>38</sup> For both proteins, the lowest surface composition of active carbohydrate that resulted in a detectable signal upon protein binding inhibition was chosen for the competition binding experiments.

**G.  $K_D$  versus  $K_{ADS}$ : A Comparison of the Multivalent Scatchard Analysis and the Langmuir Adsorption Isotherm.** In the previous section, we employed competitive binding measurements to calculate  $K_D$ , the dissociation constant for ligand–protein interactions in solution. This equilibrium constant is different than the  $K_{ADS}$  that was measured in section C for protein adsorption to the surface. Specifically, the parameter

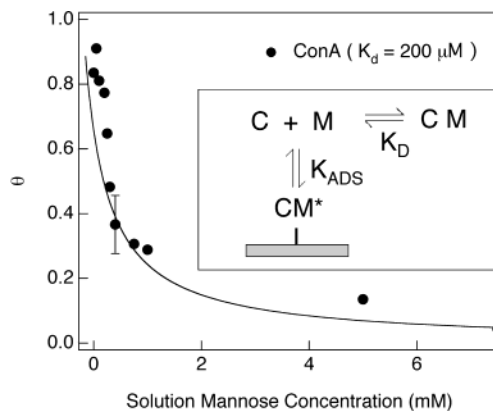


**Figure 10.** Plot of the relative surface coverage of ConA, measured with SPR imaging, as a function of the concentration of  $\alpha$ -MeMan in solution. The  $\alpha$ -MeMan in solution competes with the surface immobilized mannose through a coupled equilibrium shown in the figure inset. The figure inset has been simplified to show ConA binding to one mannose molecule from solution; however, ConA has four mannose binding sites. The data are fit as discussed in the text, using eqs 5 and 6.

$K_{ADS}^{-1}$  is the protein concentration at which half of the surface-binding sites are occupied with protein, and  $K_D$  is the ligand concentration at which half the protein-binding sites are occupied with ligand in solution. In the Experimental Methods section, the multivalent Scatchard analysis was used to derive an equation for the equilibrium dissociation constant (eq 5), whereas an adsorption isotherm was used in Section C to characterize protein interactions with the surface. A comparison of the equations that result from the Scatchard analysis and the Langmuir adsorption isotherm illustrate the differences between the parameters  $K_D$  and  $K_{ADS}$ .

For the interaction between a monovalent ligand ( $L$ ) and a multivalent protein ( $P$ ) with  $q$  binding sites, the total concentration of bound ligand divided by the total concentration of protein is defined by Winzor et al.<sup>24</sup> as the parameter  $r_f$

$$r_f = \frac{[L_o] - [L]}{[P_o]} \quad (7)$$

where  $[L_o]$  is the total concentration of ligand,  $[L]$  is the concentration of free ligand, and  $[P_o]$  is the total concentration of protein in the system. The assumptions for the analysis presented here are the same as those listed previously. Equation 7 can be rewritten in terms of the total  $[A_o]$  and free  $[A]$  acceptor site concentrations considering that (i)  $[A_o] = q[P_o]$ ; (ii)  $[A_o] = [A] + [LA]$ ; and (iii)  $[L_o] = [L] + [LA]$

$$r_f = \frac{[A_o] - [A]}{[A_o]/q} = q \left[ 1 - \frac{[A]}{[A_o]} \right] \quad (8)$$

Rearrangement of eq 3 to obtain an equation for  $[A]/[A_o]$

$$\frac{[A]}{[A_o]} = \frac{1}{1 + K_D^{-1}[L]} \quad (9)$$

and substitution of eq 9 into eq 8 yields

$$r_f = q \left[ \frac{K_D^{-1}[L]}{1 + K_D^{-1}[L]} \right] \quad (10)$$

The parameter  $r_f$  is the average number of occupied ligand

binding sites on a protein molecule in solution. Equation 10 has the same functional form as the Langmuir adsorption isotherm (eq 6 with  $a = 0$ )

$$\theta = \frac{K_{\text{ADS}}[\text{P}]}{1 + K_{\text{ADS}}[\text{P}]} \quad (11)$$

where  $\theta$  is the fraction of surface sites occupied with protein molecules, and  $K_{\text{ADS}}$  is the adsorption coefficient. Equations 10 and 11 quantitatively show the difference between  $K_{\text{D}}$  and  $K_{\text{ADS}}^{-1}$ . A comparison of the  $K_{\text{D}}$  ( $16 \mu\text{M}$  and  $200 \mu\text{M}$  for jacalin and ConA, respectively) and the  $K_{\text{ADS}}^{-1}$  ( $45 \text{ nM}$  and  $180 \text{ nM}$  for jacalin and ConA, respectively) values shows that although the adsorption coefficients can be used to rank the carbohydrate-lectin interaction strengths in solution, they cannot be used to determine directly the solution  $K_{\text{D}}$  values.

### Conclusions

We have shown that SPR imaging can be used to study characteristically weak protein-carbohydrate interactions, and that this method provides the means to assess the carbohydrate binding selectivity of lectins. SPR imaging can be used to quantitate the strength of lectin-carbohydrate interactions by determining the adsorption coefficients and the solution dis-

sociation constants for the lectins ConA and jacalin. These studies also highlight the utility of changing the ligand density on gold films as a tool to study multivalent interactions. We anticipate that the methods for fabricating carbohydrate arrays via the disulfide attachment chemistry combined with SPR imaging will facilitate the study of protein-carbohydrate interactions. We envision these methods will be useful for characterizing the sugar binding specificities of lectins and antibodies, identifying glycomimetics, and in carrying out high-throughput assays for the discovery of compounds that enhance or disrupt lectin-carbohydrate interactions.

**Acknowledgment.** This research is funded by the NSF (Grant CHE-0133151 to R.M.C.), the Defense Advanced Research Projects Agency (DARPA) and the Air Force Research Laboratory, Air Force Material Command, USAF, (F30602-01-2-0555 to R.M.C.), the NIH (Grant GM59622 to R.M.C.), and (Grant GM49975 to L.L.K.). We thank the W.M. Keck Foundation for support.

**Supporting Information Available:** Complete synthesis and characterization details for compounds 1 and 2. This material is available free of charge via the Internet at <http://pubs.acs.org>.

JA034165U